THE JOURNAL OF BIOLOGICAL CHEMISTRY VOL. 291, NO. 29, pp. 15292–15306, July 15, 2016

Tail-anchored Protein Insertion in Mammals

*FUNCTION AND RECIPROCAL INTERACTIONS OF THE TWO SUBUNITS OF THE TRC40 RECEPTOR**

Received for publication, December 4, 2015, and in revised form, May 3, 2016 Published, JBC Papers in Press, May 23, 2016, DOI 10.1074/jbc.M115.707752

Sara Francesca Colombo[‡1], Silvia Cardani[‡], Annalisa Maroli[‡], Adriana Vitiello[‡], Paolo Soffientini[§], Arianna Crespi[‡], Richard F. Bram[¶], Roberta Benfante[‡], and Nica Borgese[‡2]

From the [‡]CNR Institute of Neuroscience and BIOMETRA Department, Università degli Studi di Milano and [§]IFOM, the FIRC Institute for Molecular Oncology Foundation, Milan, Italy 20100 and [¶]Mayo Clinic, Rochester, Minnesota 55905

The GET (guided entry of tail-anchored proteins)/TRC (transmembrane recognition complex) pathway for tail-anchored protein targeting to the endoplasmic reticulum (ER) has been characterized in detail in yeast and is thought to function similarly in mammals, where the orthologue of the central ATPase, Get3, is known as TRC40 or Asna1. Get3/TRC40 function requires an ER receptor, which in yeast consists of the Get1/Get2 heterotetramer and in mammals of the WRB protein (tryptophan-rich basic protein), homologous to yeast Get1, in combination with CAML (calcium-modulating cyclophilin ligand), which is not homologous to Get2. To better characterize the mammalian receptor, we investigated the role of endogenous WRB and CAML in tail-anchored protein insertion as well as their association, concentration, and stoichiometry in rat liver microsomes and cultured cells. Functional proteoliposomes, reconstituted from a microsomal detergent extract, lost their activity when made with an extract depleted of TRC40-associated proteins or of CAML itself, whereas *in* vitro synthesized CAML and WRB together were sufficient to confer insertion competence to liposomes. CAML was found to be in ~5-fold excess over WRB, and alteration of this ratio did not inhibit insertion. Depletion of each subunit affected the levels of the other one; in the case of CAML silencing, this effect was attributable to destabilization of the WRB transcript and not of WRB protein itself. These results reveal unanticipated complexity in the mutual regulation of the TRC40 receptor subunits and raise the question as to the role of the excess CAML in the mammalian ER.

Whereas most membrane proteins are targeted to the endoplasmic reticulum (ER)[3] by the signal recognition particle-dependent co-translational mechanism (1, 2), tail-anchored (TA) membrane proteins are inserted into all their target membranes, including the ER, by post-translational pathways (for review see Refs. 3–5). The inability of TA proteins to utilize the co-translational route is due to the location of their sole targeting determinant, the transmembrane domain (TMD), at their extreme C terminus, such that it becomes accessible to cytosolic targeting factors only after release of the completed polypeptide chain from the ribosome.

Because TA proteins are numerous (6), play fundamental physiological roles (*e.g.* as SNAREs and apoptosis regulating factors; Ref. 3), and are present in all domains of life (7), a great deal of research has been dedicated to the elucidation of the mechanisms by which they reach and insert into their target membranes. On the basis of studies in cell-free mammalian systems (8, 9) and of *in vitro* and *in vivo* investigations in yeast (10), a novel system operating in the delivery of TA proteins to the ER membrane was identified and extensively characterized (for review, see Refs. 11 and 12). This system is centered around a cytosolic P-type ATPase, named Get3 (guided entry of tail-anchored proteins) in yeast and TRC40 (transmembrane domain recognition complex subunit of 40 kDa) or Asna1 (arsenical pump-driving ATPase protein) in mammals (in this paper, we refer to the mammalian protein as TRC40).

Get3-mediated delivery of TA proteins to the ER has been especially well characterized in yeast. The three-dimensional structures of many of the components have been determined, and the entire pathway has been reconstituted from purified components (for review, see Refs. 11–13). Upon release from the ribosome, the TA substrate is captured by a pre-targeting complex (12, 14), which delivers it to the Get3 ATPase. The latter is a homodimer and when bound to ATP assumes a closed conformation that presents a composite hydrophobic groove across the dimer interface (15, 16) capable of accommodating the TMD of ER-directed TA proteins (17). Get3 binds the pre-targeting complex in this ATP-bound conformation, primed to receive the TA substrate. The resulting TRC40-TA complex is

* This work was supported by the People Programme (Marie Curie Actions) of the European Union's Seventh Framework Programme FP7/2007–2013 under REA Grant 607072. See The Tampting Network for further details. This work reflects only the author's views; the union is not liable for any use that may be made of the information contained therein. The authors declare that they have no conflicts of interest with the contents of this article.

[1] To whom correspondence may be addressed: Tel.: 3902-50316971; E-mail: s.colombo@in.cnr.it.

[2] To whom correspondence may be addressed: Tel.: 3902-50316947; E-mail: n.borgese@in.cnr.it.

[3] The abbreviations used are: ER, endoplasmic reticulum; b_5, cytochrome b_5; b_5-Syb2, cytochrome b_5 with the transmembrane domain of synaptobrevin-2; CAML, calcium modulating cyclophilin ligand; DBC, Deoxy Big Chap; DS, Down syndrome; Get, guided entry of tail-anchored proteins; PC, phosphatidylcholine; PK, protease K; PrL, proteoliposome; TA, tail-anchored; TB, translocation buffer; TMD, transmembrane domain; TRC40, transmembrane recognition complex subunit of 40 kDa; WRB, tryptophan-rich basic protein; WRBcc, coiled-coil domain of WRB; qPCR, quantitative PCR; MBP, maltose-binding protein; NBD, 12-(*N*-methyl-*N*-(7-nitrobenz-2-oxa-1,3-diazol-4-yl)); CHX, cycloheximide; Tricine, *N*-[2-hydroxy-1,1-bis(hydroxymethyl)ethyl]glycine (systematic); MR, microsomes.

then released from the pre-targeting complex and recruited to the ER receptor.

The yeast ER receptor is composed of two subunits known as Get1 and -2 (10, 18). These are integral membrane proteins that are associated with 2:2 stoichiometry via their TMDs and whose expression levels are mutually interdependent. Get2, which contains a flexible cytosolic N-terminal domain, serves as tethering factor to capture the Get3-TA complex, whereas Get1, by inserting its cytosolic coiled-coil domain into the homodimer, disrupts the hydrophobic groove, causing release of nucleotide and delivery of the TA substrate to the bilayer (19–21).

Because structural or functional homologues of all components of the Get system are present in mammals and some of the central components of the pathway are interchangeable between yeast and higher eukaryotes (16, 22), it is thought that the entire Get pathway is conserved in higher eukaryotes (for review, see Refs. 3 and 4). Nevertheless, the mammalian system is much less characterized than its yeast counterpart, and several important questions remain to be addressed.

One goal that has not yet been attained in mammals is the full characterization of the TRC40 ER receptor. Although Get1 has a mammalian homologue known as WRB (tryptophan-rich basic protein), a structural homologue of Get2 has not been identified in animals. However, pulldown experiments with TRC40 as bait identified CAML (calcium modulating cyclophilin ligand) as a TRC40- and WRB-interacting protein (23). siRNA-mediated depletion of CAML or WRB partially inhibits insertion of *in vitro* translated TA proteins into the ER of semi-intact cells (23), and the WRB-CAML complex can restore function of the Get system in yeast cells deleted for the Get1/2 complex (22). Thus, CAML is considered to be the functional equivalent of Get2. However, the TRC40 pathway has not been reconstituted with purified components, so that the participation of other components in addition to those identified so far cannot be excluded. Furthermore, it is not known whether the many previously reported functions of CAML, in development, signaling, and regulation of the immune system (24–26), are or are not mere consequences of CAML's role in TA protein insertion. The stoichiometry of the CAML-WRB complex has not been defined, but it has been reported that overexpression of each subunit alone impairs TA protein insertion by the endogenous receptor (23), suggesting that, like in yeast, the two subunits are in a strict stoichiometric relation.

Here we report that CAML and WRB are sufficient to confer to liposomes the capacity to support TRC40-dependent TA protein insertion but that an excess of one subunit over the other one does not decrease this capacity either in reconstituted proteoliposomes or in Down syndrome cells in which WRB expression is increased 1.5-fold. We further find that, at variance with the situation in yeast, CAML is present in an ~5× molar excess over WRB both in rat liver microsomes and in tissue culture cells. Notwithstanding this stoichiometric imbalance, knockdown of each receptor subunit decreases the levels of the other one. Unexpectedly, however, we find that CAML affects WRB levels by stabilizing the WRB transcript rather than the WRB protein itself, revealing a novel mechanism of regulation of TRC40 receptor subunit expression.

Experimental Procedures

Plasmids—pGEM4 plasmids coding for b_5 with a C-terminal opsin tag (b_5-ops28) and for b_5 with the TMD of synaptobrevin 2 and a C-terminal opsin tag (b_5-TMSyb2-ops28), both under the SP6 promoter, have been described in previous publications (27, 28). We refer here to the encoded proteins as b_5 and b_5-Syb2. The plasmids pGEX-AT-2-NCAML and pCLX31.1-CAML, which code for GST fused to the N-terminal cytosolic portion of CAML and for FLAG tagged human CAML, respectively, are described in Tran *et al.* (24). The pQE80-MBP-WRBcc plasmid, which codes for a fusion protein between maltose-binding protein and the coiled-coil cytosolic domain of WRB (29), was a kind gift of Fabio Vilardi.

The complete coding sequence of WRB was amplified by RT-PCR from a total RNA sample prepared from IMR32 cells using Superscript reverse transcriptase (Life Technologies) and random hexanucleotide primers. WRB was amplified from the resulting cDNA using *Pfu* DNA polymerase (Promega) (upper primer: 5′-ATGAGCTCAGCCGCGGCCGACCACT-3′); lower primer: 5′-TGTTCAGCTGAACGGATGAAGCACAA-3′). The resulting amplified 524-nucleotide fragment was cloned into the pCR blunt vector (Invitrogen), excised with EcoR1, ligated into the pGEM4 vector under the SP6 promoter, and checked by sequencing.

The full-length human CAML sequence was amplified from the pCLX31.1-CAML vector (upper primer: GGTACCAG-GATGGAGTCGATGGCCGTC); lower primer: AAGCTTT-CATGGTACTTCAGAGCCCCA) using Deep Vent polymerase (New England Biolabs). The amplified fragment was ligated into the pCR blunt vector, excised with HindIII and KpnI, and subcloned into the pGEM4 vector under the SP6 promoter.

Antibodies—Polyclonal anti-TRC40 and anti-CAML antibodies produced in our laboratories have been described in previous studies (28, 30). In the case of anti-TRC40, we used two different antisera: antiserum 1 was raised against a peptide (DQKFSKVPTKVKGYDNL) corresponding to residues 84–100 of TRC40; affinity-purified antibodies from this antiserum were used for immunoblotting. Antiserum 2 was raised against a peptide (LEPYKPPSAQ) corresponding to residues 339–348 of TRC40; affinity-purified antibodies from this antiserum were used for immunodepletion of microsomal extracts.

Monoclonal antibodies (mAbs) against tubulin (clone B-5-1-2) and β-actin (clone AC-74) were from Sigma. Protein disulfide isomerase mAbs (clone 1D3) were from Enzo Life Sciences. Anti-opsin mAb R2–15, anti-ribophorin serum, and affinity-purified polyclonal anti-calnexin antibodies were kind gifts of Paul Hargrave (31), Gert Kreibich (32), and Ari Helenius (ETH, Zuerich, CH), respectively. Rabbit antiserum and affinity-purified antibodies against the coiled-coil domain of WRB were produced by Synaptic Systems in the context of a collaborative grant. When tested in Western blot against a sample of *in vitro* translated WRB, the antiserum revealed a band of the expected M_r, which was not present in a parallel sample incubated without the transcript (data not shown). In some experiments, anti-WRB mAbs from Sigma (clone2A3) at a 1:200 dilution were used. Peroxidase-conjugated anti-rabbit and anti-mouse IgG

were from Sigma, and anti-mouse IRDye 680 and anti-rabbit IRDye 800 from LI-COR Bioscience.

Cell Culture and RNA Silencing—HeLa and IMR32 cells were grown in DMEM and RPMI medium, respectively, both supplemented with antibiotics under a 5% CO_2 atmosphere. Primary skin fibroblasts, obtained from skin biopsies of euploid and chromosome 21 trisomic (Down syndrome) human fetuses, were a kind gift of Lucio Nitsch (University of Naples Federico II) (Table 1). The fibroblasts were grown in DMEM supplemented with antibiotics and 10 ng/ml FGF under a 10% CO_2 atmosphere. The cells were used for immunoblotting, qPCR, or functional assays after 5–10 passages.

For WRB or CAML silencing, HeLa cells at ~30% confluence were transfected with RNAi duplexes with the use of RNAiMAX Lipofectamine reagent (Invitrogen). WRB and CAML were silenced with two different duplex siRNAs each [Ambion Silencer select siRNAs, the sequence of the sense strand is given for each duplex: s14905 (WRB siRNA1: 5′-CAGUCAACAUGAUGGACGAtt-3′); s14906 (WRB siRNA2: 5′-GGGUGAUAAGUGUCGCUUUtt-3′); s2370 (CAML siRNA1: 5′-GCACUUCUAUUGUCGGGAAtt-3′); s2372 (CAML siRNA2: 5′-GCGCGGAAGAAGAAAGUCAtt-3′)] at a concentration of 5 nM. Parallel cultures were transfected with equal concentrations of Silencer select negative control RNA. Six hours after transfection the medium was replaced with complete growth medium; cells were collected and analyzed 48 or 72 h after transfection.

Preparation of Recombinant Proteins—The cytosolic domain of CAML (N-CAML) was produced as fusion protein in BL21 bacteria and purified by standard procedures. After thrombin digestion of the fusion protein bound to glutathione-Sepharose 4B (GE Healthcare), the released N-CAML was recovered.

MBP-WRBcc was purified from the soluble fraction of an induced BL21 sonicate. The BL21 cells, obtained from 50 ml of culture, were suspended in 2 ml of sonication buffer (200 mM NaCl, 20 mM Tris-Cl, pH 7.5, 1 mM EDTA, 1 mM DTT, 1 mM PMSF), and the cells were lysed by sonication. The soluble fraction was diluted 1:5 in the same buffer and incubated for 2 h at 4 °C with 3 ml of packed Amylose resin (New England BioLabs).

To cleave the WRBcc from MBP, the resin was incubated with GST-tagged tobacco etch virus protease, and the eluted protein was recovered after sedimentation of the amylose beads. The protease was then eliminated by incubation of the digested sample with glutathione-Sepharose 4B.

The purified recombinant proteins were used as standards for the determination of WRB and CAML concentration in microsomes, cultured cell lysates, and *in vitro* translated samples. The concentrations of the recombinant protein standards in the final solutions were determined after correcting for the presence of contaminants detected by SDS-PAGE/Coomassie staining (see Fig. 4*A*). The bicinchoninic acid and the Bradford assays, with bovine serum albumin as standard, yielded similar values.

Preparation of Rat Liver Microsomes and Microsomal Extract—Total rat liver microsomes (MR) were prepared from whole homogenates by differential centrifugation. Briefly, livers were homogenized in 5 volumes of an ice-cold solution 0.25 M sucrose, 0.1 mM EDTA, 5 mM Tris-Cl, pH 7.5, supplemented with a mixture of protease inhibitors; nuclei and mitochondria were removed by three successive centrifugations at 1,000, 9,200, and 21,000 × *g*, each for 10 min. Microsomes were sedimented from the 21,000 × *g* supernatant by centrifugation at 170,000 × *g* for 1 h. The MR were resuspended in the homogenization solution and stored in small aliquots at −80 °C. The 170,000 × *g* supernatant (cytosolic fraction) was also stored.

A microsomal detergent extract was prepared by incubating the MR (at ~8 mg protein/ml) with 0.8% Deoxy Big Chap (DBC) for 30 min on ice. The sample was then centrifuged at 100,000 × *g* for 1 h, and the supernatant was used for reconstitution experiments.

Immunodepletion of Microsomal Extract and Elution of Antibody-bound Molecules—To deplete TRC40 and the associated proteins, the microsomal extract deriving from 12 mg of total microsomal protein (in 0.6% DBC) was incubated with 0.3 mg of affinity-purified anti-TRC40 antibodies (antiserum 2) immobilized to 100 μl of packed Protein A-Sepharose beads (GE Healthcare) by dimethyl pimelimidate-mediated cross-linking (33). After incubation overnight at 4 °C, the resin was removed by centrifugation, and the supernatant (flow-through fraction) was used for analysis and reconstitution experiments. To recover the proteins bound to the immobilized antibody, the resin was incubated with an equal volume of translocation buffer (TB = 50 mM Hepes-K, pH 7.2–7.4, 250 mM sorbitol, 70 mM K^+OAc, 5 mM K^+EDTA, 2.5 mM $Mg^{2+}(OAc)_2$) containing 1 mM antigenic peptide + 0.6% DBC. After incubation for 1 h on a rocking platform, the eluted fraction was recovered by centrifugation.

CAML and associated proteins were depleted from the microsomal extract with the use of affinity-purified anti-CAML polyclonal antibodies immobilized on protein A-Sepharose, as described for TRC40 depletion. Control immunodepletions were carried out under similar conditions but using unrelated rabbit IgGs (Sigma) as the immunoadsorbent to obtain a control flow-through fraction.

Preparation of Liposomes and Proteoliposomes—Proteoliposomes (PrLs) were reconstituted from the flow-through fractions (ΔTRC40, ΔCAML, or control flow-through fraction) to obtain depleted and complete PrLs by removal of detergent with BioBeads SM-2 (Bio-Rad). Samples deriving from 0.7 mg of total microsomal protein were reconstituted in a total volume of 250 μl of TB containing 0.8% DBC, 200 μg of bovine liver phosphatidylcholine (PC; from Avanti Polar Lipids), and 300 μg of Bio-Beads SM-2, rehydrated according to the specifications of the manufacturer. To monitor recovery, NBD-labeled PC (NBD C_{12}-HPC from Invitrogen) in a 1:100 molar ratio to the added PC was included in the reconstitution mixtures. To produce replenished PrLs, the ΔTRC40 flow-through was combined with eluted fraction deriving from 1.9 mg of microsomal protein. After incubation of the samples overnight in glass vials on a rocking platform at 4 °C, the Bio-Beads were discarded; the detergent-free solution was diluted 4-fold with water and centrifuged at 200,000 × *g* for 1 h at 4 °C to recover the reconstituted proteoliposomes.

To reconstitute proteoliposomes with the eluted fraction alone or with proteins translated *in vitro* in wheat germ extract, the eluted fraction deriving from 1.9 or 3.8 mg of total micro-

somal protein or 70 μl of wheat germ extract containing *in vitro* translated WRB or CAML were incubated in a total volume of 200 μl containing 1 mg of PC + NBD-PC, salts (0.8 M KOAc, 50 mM Hepes-K^+, pH 7.5, 5 mM $Mg(OAc)_2$), 15% glycerol, 1% DBC, and 215 μg of Bio-Beads. The samples were incubated, and the proteoliposomes were recovered as described above.

The PrLs obtained by both procedures were resuspended in 30 μl of TB + 4 mM dithiothreitol and stored at −80 °C. Three μl of liposome suspension were used for 10-μl translocation reactions.

In Vitro Transcription/Translation and Translocation Assay—b_5 and b_5-Syb2 transcripts were translated in rabbit reticulocyte lysate (from Green Hectares) in the presence of [^{35}S]methionine (change to PerkinElmer Life Sciences, translation grade) according to standard procedures. For the experiments with semi-intact fibroblasts (see below), translation was carried out with unlabeled methionine in the absence of the radioactive amino acid, and the translation products were revealed by Western blotting with anti-opsin antibodies. In all cases translation was blocked by the addition of 300 μg/ml cycloheximide (CHX, Sigma), and ribosomes were removed before carrying out post-translational insertion assays.

WRB and CAML were translated in wheat germ extract (Promega) in the presence of nonradioactive methionine according to the instructions of the manufacturer. The solubility of the translated proteins was checked by ultracentrifugation. ~50% of both proteins remained in the supernatant after centrifugation at 150,000 × *g* for 1 h, a percentage that was not changed by the addition of DBC.

Translocation of the C terminus of TA proteins into MR, liposomes or reconstituted PrLs was monitored by a protease protection assay as previously described (34). Protected fragments were isolated by immunoprecipitation with anti-opsin antibodies.

Integration of TA proteins into the ER of semi-intact primary fibroblasts was monitored by evaluating the percentage of glycosylation of the C-terminal opsin epitope. The fibroblasts, grown to ≥80% confluence in 12-well multiwell plates, were washed twice with import buffer (0.25 M sucrose, 2.5 mM $Mg^{2+}(OAc)_2$, 25 mM KCl, 1 μM taxol, 20 mM Hepes-K^+, pH 7.4), incubated at 26 °C for 5 min in the same buffer containing 25 μM digitonin (Calbiochem), washed 2 times with import buffer, and then exposed to 300 μl of rabbit reticulocyte lysate containing the *in vitro* translated substrate and supplemented with 1 μM taxol and 1 mM glutathione. After incubation at 26 °C for 1 h, the cells were washed twice with KHM buffer (110 mM K^+OAc, 2 mM $Mg^{2+}(OAc)_2$, 1 μM taxol, 20 mM Hepes-K^+, pH 7.4) and then lysed with 100 μl of preheated SDS lysis buffer (1% SDS, 0.1 M Tris-Cl, pH 8.9, supplemented with protease inhibitors).

qPCR—Total RNA was prepared with the use of the RNeasy™ Mini kit or RNA plus micro kit and accompanying QIAshredder™ (Qiagen, Hilden, Germany) according to the instructions of the manufacturer. 1 μg of RNA was retrotranscribed with reagents of the SuperScript IV reverse transcriptase kit from Invitrogen. Quantification of WRB, CAML, and GAPDH transcripts was carried out by qPCR using Taqman probes, designed by Life Technologies in an ABI-PRISM Thermocycler (QuantStudio 5). The assays were CAMLG (ID #Hs00266143_m1) and WRB (ID #Hs00190294_m1); glyceraldehyde-3 phosphate dehydrogenase (GADPH; ID#Hs99999905_m1) was used as the internal standard after its compatibility with the other assays had been confirmed. Each sample was run in triplicate, and the results were calculated using the $2^{-\Delta CT}$ and the $2^{-\Delta\Delta CT}$ see "Experimental Procedures" to allow the normalization of each sample to the internal standard and comparison with the calibrator of each experiment (set to a value of 1) as described in the figure legends. To analyze transcript stability, cells were treated with 60 μM DRB (Sigma), and RNA was extracted at the times indicated in the figure legend.

Miscellaneous Techniques—Protected fragments were analyzed on Tris-Tricine SDS gels as previously described (34). Dried gels were imaged with Storm phosphorimaging (GE Healthcare), and band intensities were quantified with ImageQuant software.

Blotting onto nitrocellulose or polyvinylidene difluoride filters and subsequent immunostaining of the blots was carried out by standard procedures. To analyze protein stability, cells were treated with 50 μg/ml CHX and lysed at the times indicated in the figure legends.

Primary antibodies were generally revealed by infrared-conjugated IgG IRDye (LI-COR Bioscience) and scanned with the Odyssey CLx Infrared Imaging System; band intensities were determined with Image Studio software (LI-COR Biosciences). Statistical analysis was carried out with the use of Prism v. 5.0 software. Details are given in the figure legends.

Results

Characterization of Proteoliposomes Functional in TA Protein Insertion—As a first step toward the biochemical dissection of the insertion step of TA proteins into the mammalian ER, we generated reconstituted PrLs from a microsomal detergent extract and probed their function in TA protein insertion.

The detergent DBC is known to yield a pancreatic rough microsomal extract that is functional in Sec61-dependent translocation (35, 36). We used this same detergent to prepare an extract from rat liver MRs. After removal of DBC-insoluble material by centrifugation, PrLs were generated by Bio Bead-mediated depletion of the detergent from the supernatant. The PrLs were then assayed for the insertion of a TRC40-independent and a TRC40-dependent substrate: cytochrome b_5 (b_5), and b_5 with its TMD replaced with the more hydrophobic one of synaptobrevin 2 (b_5-Syb2), respectively (27, 28). Both constructs contain at their extreme C terminus an epitope (derived from the N-terminal region of bovine opsin), which confers an *N*-glycosylation site and recognition by an anti-opsin mAb. As shown in Fig. 1*A*, both constructs were able to translocate their C terminus across microsomal membranes, as demonstrated by glycosylation (*arrows*) and generation of glycosylated and non-glycosylated protected fragments after exposure of the completed translocation reaction to protease K (*lane 3*, *+PK*). When the reaction was carried out with PrLs instead of microsomes, glycosylation was no longer detected, as expected (34), but translocation of the C terminus could still be demonstrated by the generation of a PK-resistant fragment (*lane 5*). A similar

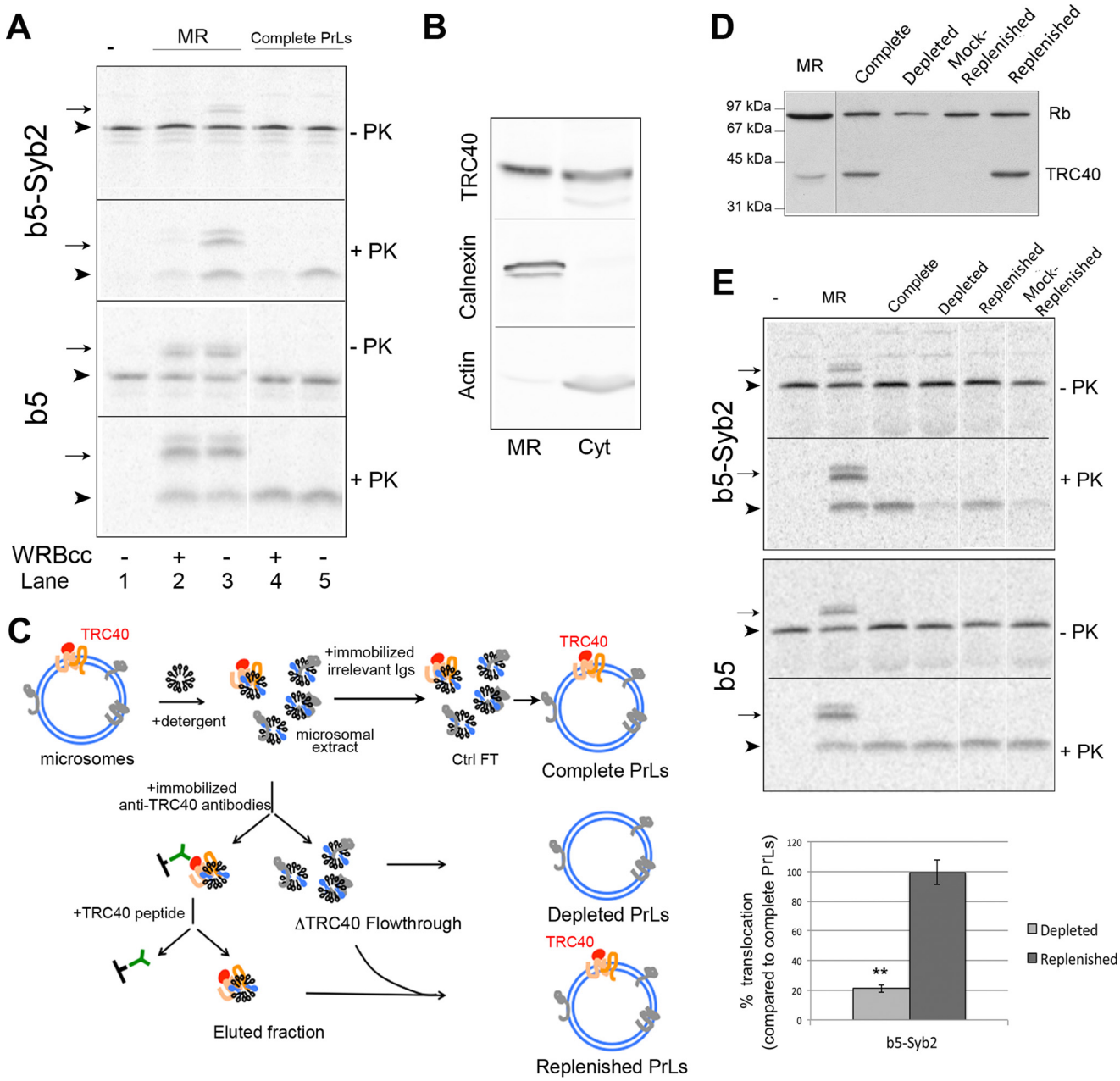

FIGURE 1. **Microsomal extracts depleted of TRC40-associated components fail to support TRC40-dependent TA protein insertion.** A, b_5 or b_5-Syb2, translated *in vitro* in rabbit reticulocyte lysate were incubated further in the presence of cycloheximide either without additions or in the presence of MRs or reconstituted PrLs. Where indicated, WRBcc was added at 5 μM concentration. At the end of the insertion reaction, $^1/_{10}$ of the samples were analyzed directly (−*PK*) and the rest digested with PK. The +PK panels show the generated protected fragments. The *arrow* and *arrowhead to the left* of the *panels* indicate, respectively, the glycosylated and non-glycosylated forms of each protein and of its corresponding protected fragment (+*PK*). The *white line in the lower two panels* separate lanes that were from the same gel and exposed together. *B*, distribution of TRC40, calnexin, and actin of postmitochondrial supernatant between the MR and the high speed supernatant (*Cyt*). *C*, schematic illustration of the protocol for depleted and replenished PrL generation. *D*, TRC40 content of PrLs reconstituted with TRC40 depleted or replenished microsomal extracts; *Rb*, ribophorin. *E*, *in vitro* translated b_5 or b_5-Syb2 were post-translationally incubated without additions or with MR or PrLs, as indicated, and then digested with PK as in *panel A*. The meaning of the *arrows* and *arrowheads to the left of the panels* and of the *white lines separating the lanes* is the same as in *panel A*. The *histogram at the bottom of the panel* shows the mean translocation values for b_5-Syb2 compared with complete PrLs ± S.E. ($n = 13$; **, $p = 0.005$ for depleted *versus* replenished PrLs.

result was obtained with another TRC40-dependent substrate (Sec61β; Ref. 37)

To verify that b_5-Syb2 inserts into reconstituted PrLs via a TRC40-dependent pathway, we analyzed the effect of the recombinant coiled-coil domain of WRB (WRBcc) added to the reaction together with the TA substrate. WRBcc, by acting as decoy receptor for TRC40, inhibits the insertion into MRs of TRC40-dependent substrates (29). As shown in Fig. 1*A*, WRBcc strongly inhibited insertion of b_5-Syb2 but not of b_5, both, into MRs (*lane 2*) and into PrLs (*lane 4*). Thus, the reconstituted PrLs function in TRC40-dependent TA protein insertion.

To identify MR components involved in the insertion, we took advantage of the observation that a considerable proportion of TRC40 is associated with the pancreas ER (8). We reasoned that at least part of this might be associated with functional receptors and that, therefore, immunodepletion of

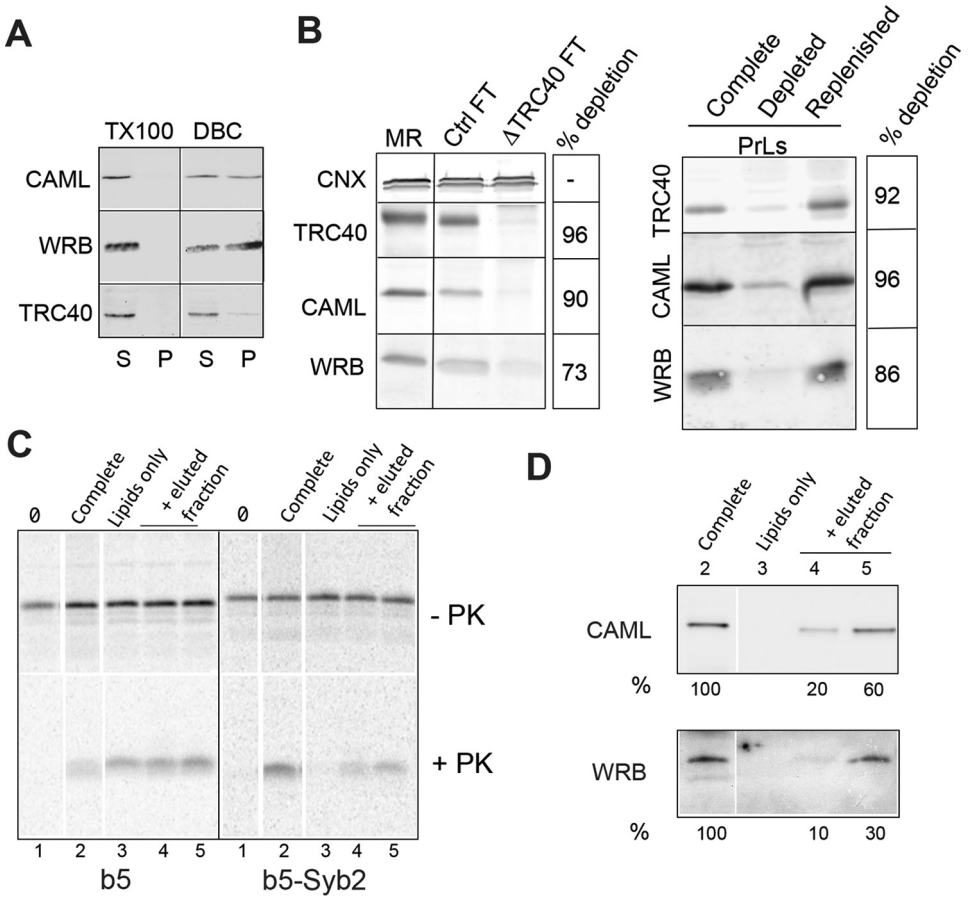

FIGURE 2. **TRC40-associated proteins are sufficient to confer insertion competence to liposomes.** *A*, partial solubilization of CAML and WRB by DBC. An MR suspension was incubated for 30 min on ice with an equal volume of Triton-X100 (2× radioimmune precipitation assay buffer)- or DBC- (2× TB + 1%DBC)-containing buffer. The samples were then centrifuged at 50,000 rpm (Beckman TLA 100.3 rotor) for 45 min. Equal aliquots of the pellets (*P*) and supernatants (*S*) were analyzed for the indicated proteins by immunoblotting. *B*, *left*, a microsomal DBC extract was incubated with immobilized anti-TRC40 or irrelevant (*Ctrl*) antibodies. The unbound fractions (flow-through (*FT*)) were analyzed for the indicated proteins by immunoblotting. Equal aliquots of the samples were loaded. The *gray line* separates lanes that were from the same blot and exposed together. The *numbers on the right* indicate the % of depletion of the ΔTRC40 *versus* the control flow-through. *Right*, PrLs were reconstituted from equivalent amounts of control or ΔTRC40 FT to generate complete or depleted PrLs. Replenished PrLs were generated by combining the ΔTRC40 FT with the eluted fraction (see "Experimental Procedures"). The *numbers on the right* indicate the % of depletion of the depleted *versus* the complete PrLs. *CNX*, calnexin. *C*, PrLs were generated from PC plus the eluted fraction (obtained from extract corresponding to 1.9 and 3.8 mg of microsomal protein, *lanes 4* and *5*, respectively) and assayed for translocation of b_5 and b_5-Syb2, in comparison with PrLs generated from the complete extract (*lane 2*), and pure lipid vesicles (*lane 3*). Translocation without added vesicles is shown in *lane 1*. *D*, immunoblot analysis of WRB and CAML content of the PrLs of *panel C*. The *numbers below the lanes* indicate the % of the indicated proteins compared with complete PrLs. In *panels C* and *D*, the *white lines* separate lanes that were from the same gel or blot and exposed together.

TRC40 from the microsomal extract might co-deplete the ER receptors as well. We first confirmed that also in rat liver a substantial portion of TRC40 is associated with MRs (Fig. 1*B*). We then set up a depletion protocol whereby PrLs were reconstituted from an extract immunoabsorbed to immobilized anti-TRC40 antibodies (ΔTRC40 flow-through) to generate depleted PrLs. The material adsorbed to the antibody-resin could be eluted with the peptide used to raise the antibodies; this eluted fraction was added back to the ΔTRC40 flow-through to obtain replenished PrLs (Fig. 1*C*). In all our experiments, the extent of depletion in the ΔTRC40 flow-through was verified by quantitation of Western blots (Figs. 1*D* and 2*B*), and only flow-through fractions depleted >90% were used to reconstitute PrLs.

As shown in Fig. 1*E*, TRC40 depletion had no effect on b_5 insertion but strongly reduced b_5-Syb2's integration. The eluted fraction combined with the ΔTRC40 flow-through fraction generated functional PrLs, whereas a fraction eluted with the same immunogenic peptide from components adsorbed to non-immune immobilized IgGs was ineffective (Mock-replenished PrLs). Thus, the eluted fraction contains components required for TRC40-mediated TA protein insertion.

Because CAML and WRB are recognized as the mammalian TRC40 receptor (22, 23, 29), we investigated whether immunoadsorption of microsomal TRC40 caused depletion of these two polypeptides. We followed the distribution of CAML, WRB, and TRC40 between the DBC soluble and insoluble MR fractions (Fig. 2*A*) and in the ΔTRC40 flow-through and control flow-through (extract exposed to immobilized non-immune IgGs) fractions (Fig. 2*B*). Although Triton-X100 solubilized all three of the proteins (Fig. 2*A*, *left*), DBC extracted nearly all of the TRC40 but only about 50% of CAML and WRB (Fig. 2*A*, *right*). Interestingly, we found that under our conditions rat microsomal Sec61α is totally insoluble in DBC, and the corresponding PrLs are consequently inactive in the co-translational translocation pathway (37).

As shown in Fig. 2*B*, *left*, depletion of TRC40 resulted in co-depletion of both CAML and WRB in the flow-through fraction, indicating that both proteins are quantitatively associated with MR-associated TRC40. Furthermore, these two proteins were reconstituted into complete and replenished PrLs but absent from the depleted vesicles (Fig. 2*B*, *right*). The presence of CAML and WRB in the eluted fraction and their absence in the ΔTRC40 flow-through was confirmed also by mass spectrometry (not shown). Thus, the presence of CAML and WRB correlates with the functional proficiency of the PrLs in TA protein insertion.

We then asked whether the components in the eluted fraction are sufficient to reconstitute functional PrLs. To this end we reconstituted the eluted fraction with pure PC. As shown in Fig. 2*C*, *right panel*, protein-free liposomes were incapable of inserting b_5-Syb2 but acquired this capacity if reconstituted with the eluted fraction. The efficiency of b_5-Syb2 integration compared with complete PrLs (Fig. 2*C*, *right panel*, *lane 5 versus lane 2*, ~30%) correlated with the extent of integration of WRB in the reconstituted PrLs (Fig. 2*D*).

To directly assess the role of CAML in reconstituted PrLs, we generated an extract depleted of CAML by incubating it with immobilized anti-CAML antibodies. As shown in Fig. 3*A*, depletion of CAML resulted in the co-depletion of WRB. Instead, a large proportion of TRC40 remained in the extract, suggesting that most of the ER-associated TRC40 is associated with ER proteins other than the WRB-CAML complex. The PrLs generated from the ΔCAML extract had severely reduced insertion competence (Fig. 3, *B* and *C*), confirming the essential role of CAML and/or CAML-associated proteins in TRC40-mediated TA protein integration.

Imbalance of CAML-WRB Stoichiometry Does Not Interfere with TA Protein Insertion—In budding yeast, Get1 and -2 are present in approximately stoichiometric amounts (19). The stoichiometry of CAML and WRB has not been investigated; however, it has been reported that overexpression of either CAML or WRB alone interferes with TA protein insertion, suggesting that single, non-functional, receptor subunits might compete with the functional heterotetrameric receptor for TRC40-TA protein complex binding (23).

We first investigated whether a stoichiometric relationship between CAML and WRB similar to yeast is present in mammalian cells. To determine the absolute amounts of the two receptor subunits in rat liver MRs, we carried out quantitative immunoblotting experiments using the recombinant proteins as standards (Fig. 4*A*). As shown in Fig. 4, *B* and *C*, we obtained a linear relationship between fluorescence signal and the amount of recombinant protein loaded on the gels. Using these standard curves, we obtained an estimated ~3 pmol/mg microsomal protein for WRB and a 4-fold higher concentration of CAML (Fig. 4*D*).

We asked whether the excess of CAML over WRB is restricted to rat liver MRs or present also in other cells. We, therefore, quantitatively determined the two proteins in whole cell lysates of IMR32 (a human neuroblastoma cell line) and in human primary fibroblasts with the same methodology used for MRs. As shown in Fig. 4, *C* and *D*, and in Fig. 6*B*, CAML was found to be in large excess over WRB (~7-fold) also in these cells.

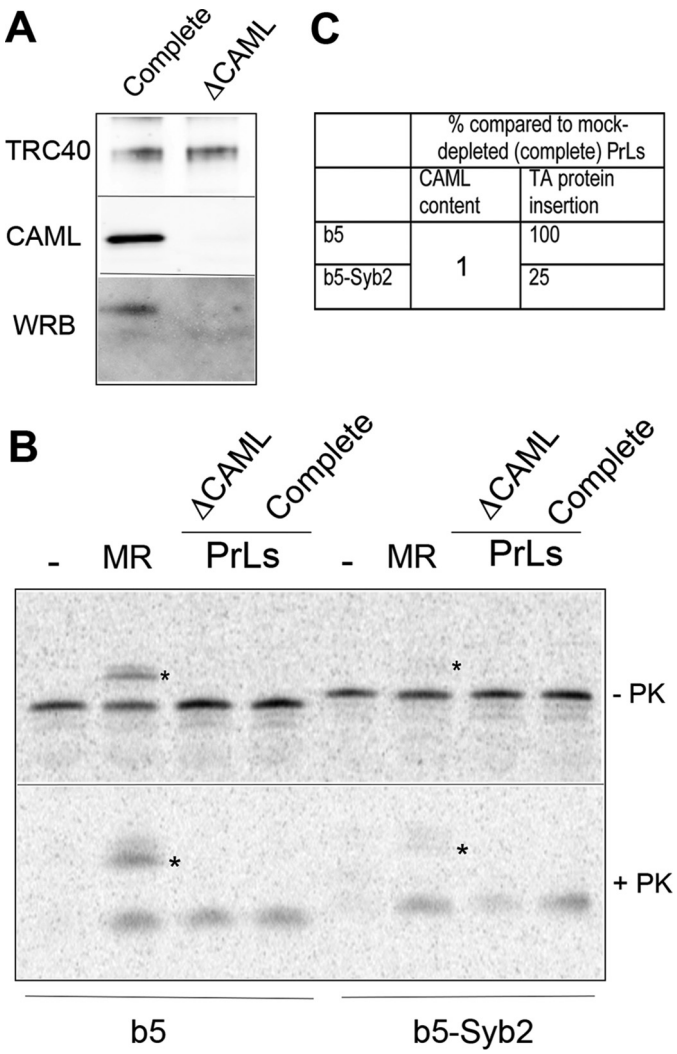

FIGURE 3. **CAML immuno-adsorption depletes WRB from the microsomal extract and reduces insertion competence of the reconstituted proteoliposomes.** *A*, PrLs reconstituted from the FT of irrelevant IgGs or anti-CAML antibodies were analyzed by immunoblotting for the indicated proteins. *B*, the same PrLs were assayed for insertion of b_5 and b_5-Syb2 by the PK protection assay. The *asterisks* indicate the glycosylated full-length proteins (−*PK*) and protected fragments (+*PK*). *C*, comparison of insertion efficiency and CAML content in CAML-depleted PrLs.

We then directly assessed the effect of unbalanced CAML to WRB ratios by incorporating known amounts of the *in vitro*-translated proteins into liposomes and testing the resulting PrLs in b_5-Syb2 translocation (Fig. 5*A*). The amounts of *in vitro* translated proteins were determined by Western blotting as done in Fig. 4. As shown in Fig. 5, *B* and *C*, liposomes made with CAML alone were about as incompetent as pure lipid liposomes in b_5-Syb2 translocation (compare *lanes 1* and *6* of Fig. 5*B*, *+PK panel*), whereas liposomes made with WRB alone did show some integration competence (Fig. 5*B*, *+PK panel*, *lane 7*). Insertion competence was better when the two proteins were incorporated in ~1:1 stoichiometry, demonstrating that CAML and WRB are sufficient to generate PrLs functional in TA protein insertion. Notably, however, the addition of an excess of either component stimulated, rather than inhibiting,

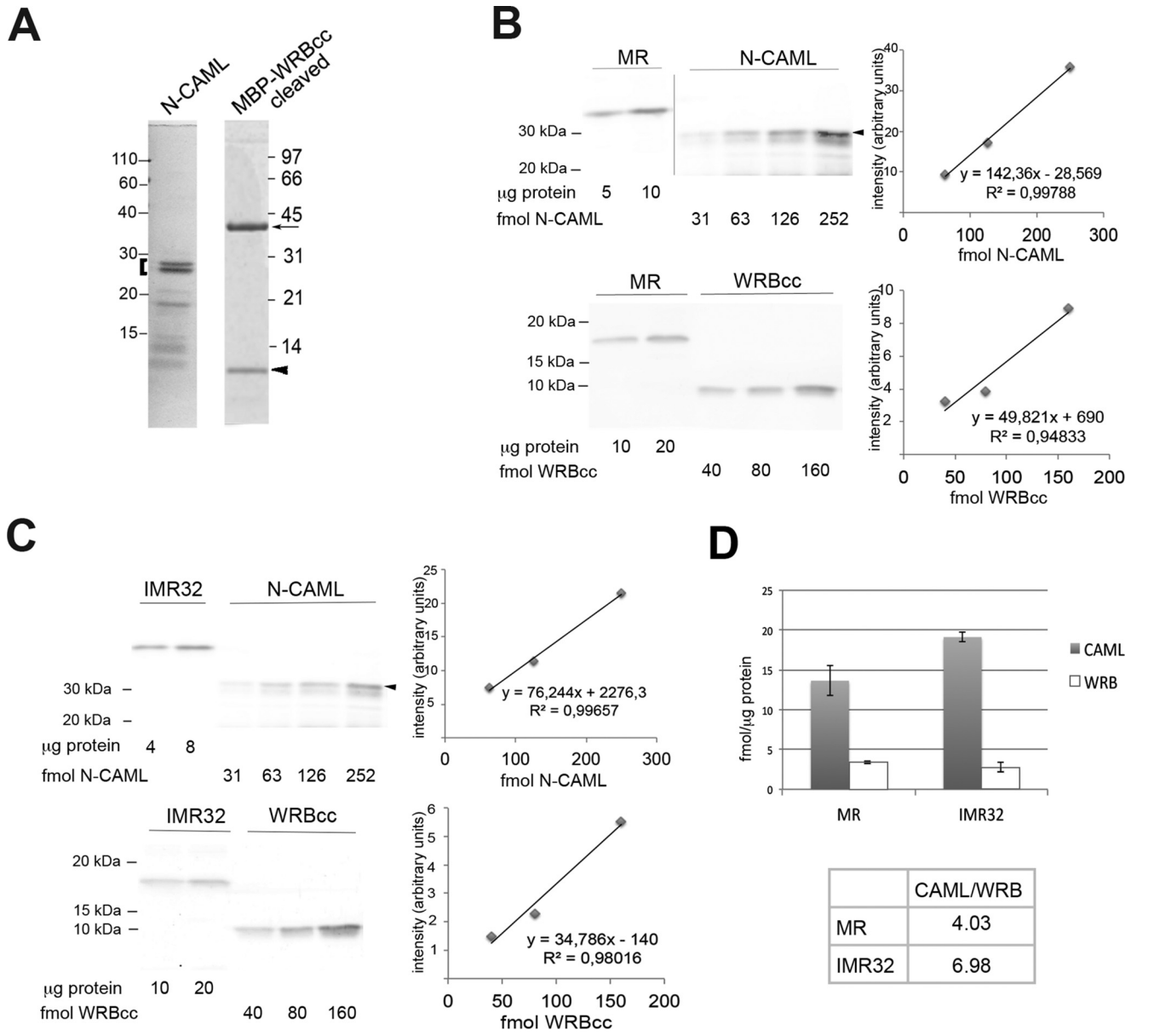

	CAML/WRB
MR	4.03
IMR32	6.98

FIGURE 4. **CAML is present in excess over endogenous WRB in rat liver microsomes and in IMR32 cells.** *A*, Coomassie-stained gels of recombinant proteins used as standards. The *bracket on the left* indicates the N-CAML doublet. The *lower bands* represent degradation products of N-CAML (23). The *arrowhead* and *arrow on the right* indicate tobacco etch virus-cleaved WRBcc and MBP, respectively. The ratio of the CAML doublet and of WRBcc to total protein in the samples was determined by densitometry. *B*, the indicated amounts of MRs were loaded alongside known amounts of recombinant CAML or WRB standard as indicated. The amounts of the endogenous proteins were determined from the standard curves shown to the *right of the panel*. The *gray line in the upper panel* separates lanes that were from the same gel or blot and exposed together. *C*, determination of CAML and WRB concentration in IMR32 cell lysates was carried out as described for *panel B*. In *panels B* and *C*, the *arrowhead* on the *right of the upper panel* indicates the full-length recombinant N-CAML band. *D*, summary of quantifications: values of CAML for MR and IMR32 are from five and three separate determinations, respectively, each with duplicate loadings ± S.E.; values of WRB for MR and IMR32 are from four and two separate determinations, respectively, each with duplicate loadings ± S.E.

TA protein integration (Fig. 5, *B*, *lanes 4* and *5*, and *C*). It must be noted, however, that the absolute amounts of *in vitro* synthesized CAML and WRB in the functional PrLs was way in excess over those present in PrLs reconstituted with the eluted fraction (Fig. 5*B*, *bottom panels*). PrLs made with lower amounts of *in vitro* synthesized receptor proteins were non-functional.[4]

To further investigate possible functional consequences of WRB to CAML imbalance, we turned to a natural cellular model, consisting in Down Syndrome (DS) fetal fibroblasts. The WRB gene is located in the distal region of the long arm of chromosome 21 (Hsa21), in a region thought to play a critical role in the Down syndrome (DS) phenotype (DS critical region) (38). WRB is among the Hsa21 transcripts reported to be 1.5-fold up-regulated in trisomic fibroblasts (39) and in DS fetal heart (40).

We first asked whether WRB transcript up-regulation also corresponds to increased protein levels, a question that had not been previously addressed. Primary fibroblasts from three DS fetuses and from four euploid controls (Table 1) were first ana-

[4] S. F. Colombo, S. Cardani, A. Maroli, A. Vitiello, P. Soffientini, A. Crespi, R. F. Bram, R. Benfante, and N. Borgese, unpublished results.

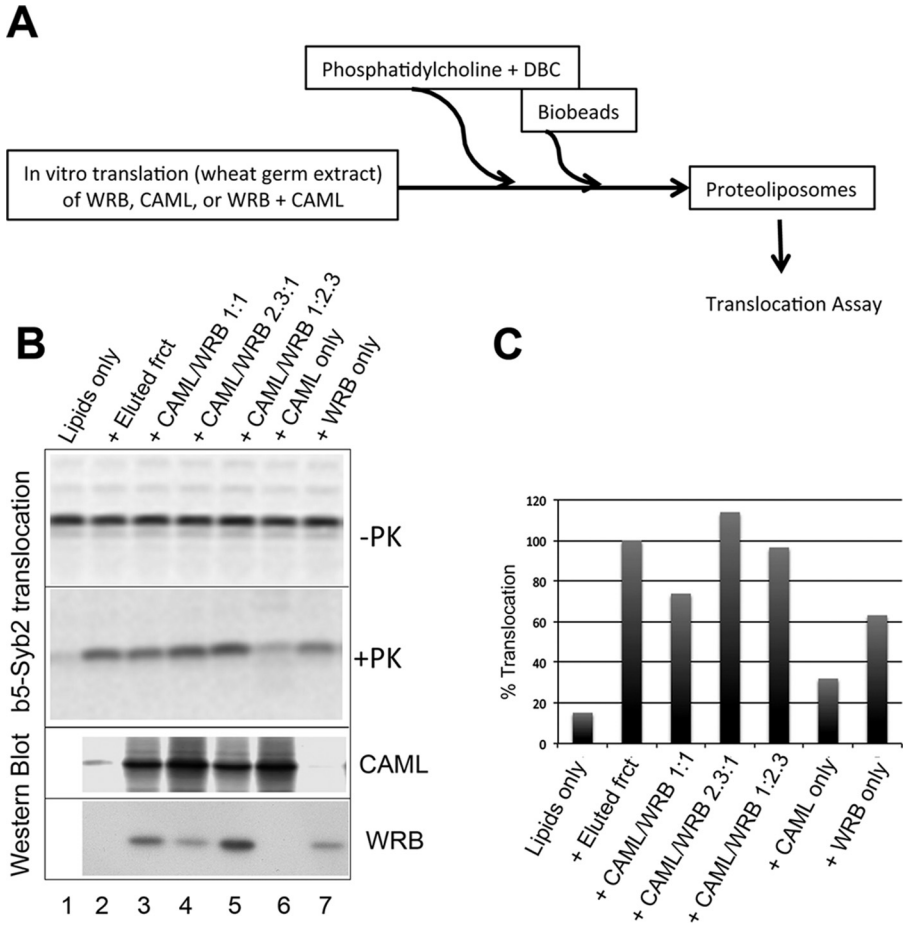

FIGURE 5. **Excess CAML does not interfere with TA protein insertion.** *A*, schematic representation of experimental setup. *B*, insertion of b_5-Syb2 into the indicated PrLs assayed by protease protection (*upper two panels*) and analysis of the same PrLs for CAML and WRB content by immunoblotting (*lower two panels*). PrLs were reconstituted with WRB and CAML translated together; in the WRB-CAML translation mix, transcript levels were adjusted to obtain equimolar amounts of the two translation products (*lane 3*, 10 pmol each). The samples of *lanes 6* and *7* were reconstituted with 10 pmol of CAML or WRB translated alone. The samples of *lanes 4* and *5* were reconstituted with 10 pmol of the CAML-WRB translation mix supplemented with either excess CAML or WRB as indicated. *frct*, fraction. *C*, quantification of the insertion assay of *panel B*.

TABLE 1
Characteristics of human primary fibroblasts used in our study

Biopsy	Karyotype	Week of gestation
70	47, XX + 21	16
71	47, XX + 21	18
77	47, XX + 21	16
79	46, XX	18
21	46, XY	21
29	46, XY	18
75	46, XX	21

lyzed by qPCR, to confirm in these subjects the up-regulation of WRB transcript and to compare CAML transcript levels in euploid and trisomic cells. As illustrated in Fig. 6*A*, CAML transcript levels of the trisomic cells were similar to those of controls, whereas WRB was significantly up-regulated (median DS/median euploid, 1.62; mean DS/mean euploid, 1.66).

Having determined that the absolute levels of WRB and CAML in the euploid primary fibroblasts were similar to those found in IMR32 and rat liver MRs (Fig. 6*B*), we compared the levels of the two proteins in trisomic *versus* euploid cultures. As shown in Fig. 6*C*, WRB levels, normalized to tubulin, were increased on average 1.8-fold (right histogram), whereas CAML levels were hardly affected (CAML levels in trisomic *versus* euploid cells, 1.16). The increase of WRB and near constancy of CAML determined a statistically highly significant increase (1.42-fold) in the WRB to CAML ratio in trisomic cells (Fig. 6*C*, *lower histogram*).

We then compared the functional proficiency in TA protein insertion of trisomic *versus* euploid fibroblasts. Semi-intact fibroblasts were incubated with *in vitro* translated b_5 or b_5-Syb2, and integration into the ER was evaluated by the extent of glycosylation of the C-terminal opsin epitope. As shown in Fig. 6*D*, ~50% of each substrate was glycosylated both in euploid and trisomic cells, indicating that the increased WRB to CAML ratio does not adversely affect TA protein integration.

Effect of WRB and CAML Levels on Each Other's Expression—In yeast, deletion of Get1 or 2 causes partial or nearly complete loss of the second receptor subunit (19, 20). To investigate whether a similar phenomenon occurs in mammals, we silenced either CAML or WRB and analyzed both proteins in the lysates prepared from the silenced cells (Fig. 7). CAML silencing was obtained with two different siRNAs, which caused ~60 and >80% reduction (siRNA1 and -2, respectively) of CAML protein levels after 48 h (Fig. 7, *panel A*). Silencing with both siRNAs caused a parallel WRB depletion, the extent of which correlated with the efficiency of CAML silencing. Sim-

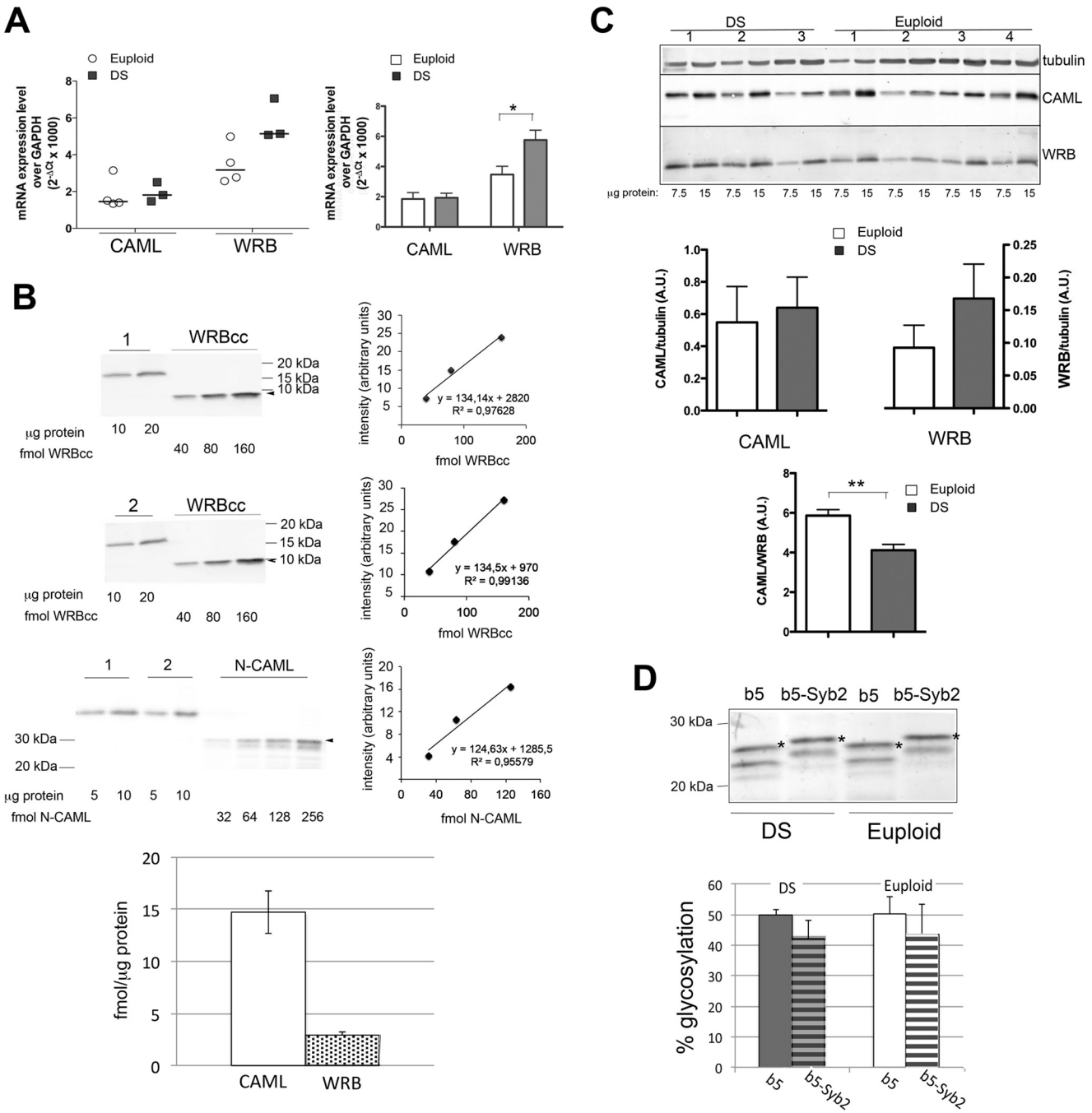

FIGURE 6. **Quantification of WRB-CAML mRNA and protein and efficiency of TA protein integration in DS *versus* euploid primary fibroblasts.** *A*, determination of CAML and WRB transcript levels in euploid and trisomic primary fibroblasts by qPCR. The *left panel* shows the single values and resulting medians; the *right panel* shows averages ± S.E. *, $p = 0.043$ by Student's two-tailed *t* test. *B*, determination of CAML and WRB concentration in two primary euploid fibroblast cultures; the procedure and symbols on the blots are as in Fig. 4. The *histogram* shows the average values from two separate determinations for each primary culture, each with duplicate loadings, ± half-range. *C*, immunoblot analysis of CAML and WRB levels in the same euploid and trisomic fibroblast cultures of *panel A*. Means of values normalized to tubulin ± S.E. are shown in the *upper two histograms*. The CAML-WRB ratio, shown in the *lower histogram* is significantly different in DS *versus* euploid cells (**, $p = 0.01$ by Student's two-tailed *t* test). *D*, integration of b_5 and b_5-Syb2 into the ER of semi-intact euploid or DS fibroblasts. Fibroblasts were permeabilized with digitonin (see "Experimental Procedures") and incubated with the *in vitro* synthesized proteins, which were revealed by Western blotting with anti-opsin antibodies. The *asterisks* indicate the glycosylated form. The histograms show the means ± S.E. ($n = 3$). No difference between euploid and DS cells was detected for either substrate.

ilarly, silencing of WRB with two different siRNAs caused a comparable reduction in CAML levels (Fig. 7, *panel B*). The levels of two ER proteins not involved in the TRC40 pathway (calnexin and protein disulfide isomerase) were not affected by either WRB or CAML silencing (*A* and *B*, third blot from the top). Interestingly, however, both WRB and CAML silencing (the latter with siRNA2) significantly reduced the levels of TRC40 expression (quantification shown in the histograms of Fig. 7, *panels A* and *B*).

To investigate at which step the TRC40 receptor subunits influence each other's expression, we analyzed the levels of the corresponding transcripts after silencing (Fig. 7, *C* and *D*). As

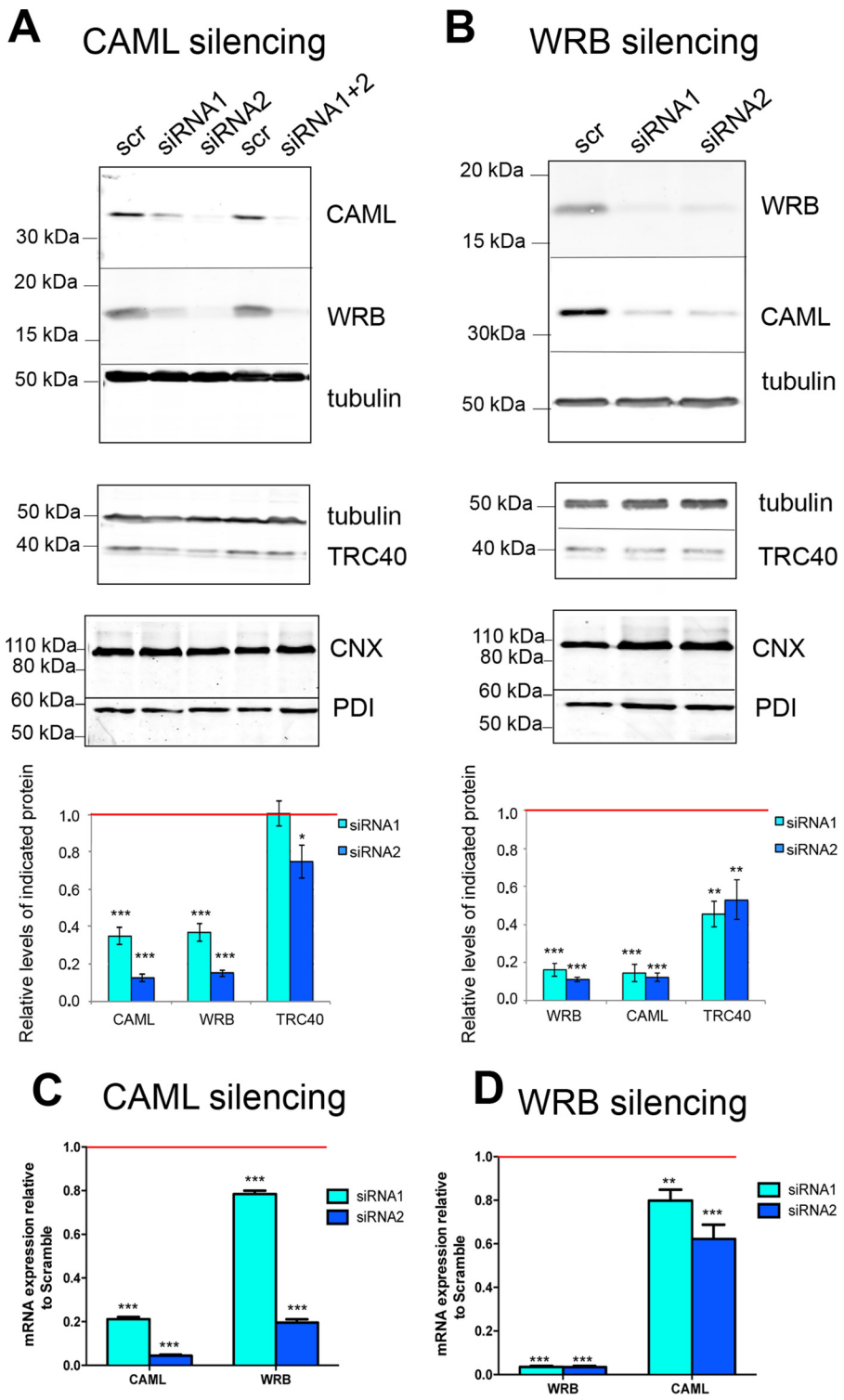

FIGURE 7. **Silencing of each TRC40 receptor subunit affects the levels of the other one as well as of the corresponding transcripts.** *A* and *B*, protein analysis. *C* and *D*, RNA analysis. Lysates were prepared from HeLa cells 48 h after transfection with CAML silencing or scrambled (*scr*) paired oligonucleotides (*A* and *C*) or 72 h after transfection with WRB silencing or scrambled paired oligonucleotides (*B* and *D*). Equal aliquots were analyzed by Western blotting (*A* and *B*) as indicated. Two unrelated ER proteins (calnexin (*CNX*) and protein disulfide isomerase (*PDI*)) were also determined. Mean values ± S.E. of CAML, WRB, and TRC40, normalized to control cells, are shown in the histograms of *panels A* and *B*. ***, **, and *, $p \leq 0.001$, 0.01, and 0.05, respectively, for the difference between siRNA and scrambled control, analyzed by repeated measures analysis of variance and Bonferroni post-analysis, after logarithmic conversion of Western blot band intensities ($n = 4$ and 5 for *panels A* and *B*, respectively). *C* and *D*, RNA prepared from cells, treated as in *A* and *B*, respectively, was subjected to retrotranscription and qPCR for the indicated transcripts. Shown are the averages of triplicate determinations ± S.D. ***, **, and *, $p \leq 0.001$, 0.01 and 0.05, respectively, for the difference between siRNA and scrambled control, analyzed by one-way analysis of variance and Bonferroni post-analysis.

expected, each oligonucleotide pair was effective against its cognate transcript, with again CAML siRNA2 more effective than siRNA1. Unexpectedly, however, silencing of each of the transcripts also reduced the levels of the other one. This effect was most marked after CAML silencing, where a >90% silencing of CAML transcript was accompanied by ≈80% down-regulation of WRB mRNA (Fig. 7*C*).

Because of the strong effect of CAML silencing on WRB transcript levels, we investigated how CAML knockdown affects WRB protein and mRNA stability. We chose to carry out these experiments after 24–28 h of silencing, a time at which both WRB protein and transcript were still detectable. To analyze protein and transcript stability, the cells were treated either with CHX or DRB, to inhibit protein synthesis or transcription, respectively, and lysed and analyzed at the times indicated in Fig. 8. As shown in Fig. 8*A*, under control conditions (scrambled oligonucleotide pair) both WRB and CAML levels were reduced by ~50% after 6 h of exposure to CHX, and this behavior was not significantly changed by CAML silencing. In contrast, as shown in Fig. 8*B*, CAML knockdown dramatically reduced the stability of WRB transcript, which was stable for up to 6 h in control cells, but rapidly degraded, with a $t_{1/2}$ of <2 h, in the CAML knockdown cells. Thus, CAML depletion affects WRB protein levels by destabilizing WRB transcript.

Discussion

In this study we have analyzed the role of the TRC40 receptor subunits, CAML and WRB, in TA protein insertion into the ER and shown that the two subunits, synthesized *in vitro*, are sufficient to confer insertion competence to phospholipid vesicles. We also find that a stoichiometric excess of one subunit over the other does not affect TA protein insertion and, in agreement, that endogenous CAML is present in an ~5-fold molar excess over endogenous WRB both in rat liver microsomes and in cultured cells. Notwithstanding this stoichiometric imbalance, the levels of each of the TRC40 receptor subunits depend critically on the presence of the other one. Unexpectedly, however, we demonstrate that CAML depletion reduces WRB levels by destabilizing the WRB transcript rather than affecting the stability of the WRB protein itself. Our findings reveal unanticipated complexities in the function and regulation of the TRC40 receptor.

Dependence of TA Protein Insertion on the TRC40/CAML-WRB Pathway—The PrLs that we generated from a rat liver microsomal extract contained approximately the same concentration of WRB and CAML as native MRs and were equally proficient in the insertion of a TRC40-dependent TA substrate. Insertion competence was nearly completely dependent on a fraction (eluted fraction) that contained TRC40-associated proteins, including CAML and WRB. Depletion of CAML itself, which caused co-depletion of WRB, but not of TRC40, also strongly compromised the insertion competence of the PrLs. These results are in substantial agreement with the conclusions of Yamamoto and Sakisaka (23), based on siRNA-mediated knockdown of CAML and WRB in cultured cells, followed by insertion assays of a TA substrate in the digitonin-permeabilized, silenced cells.

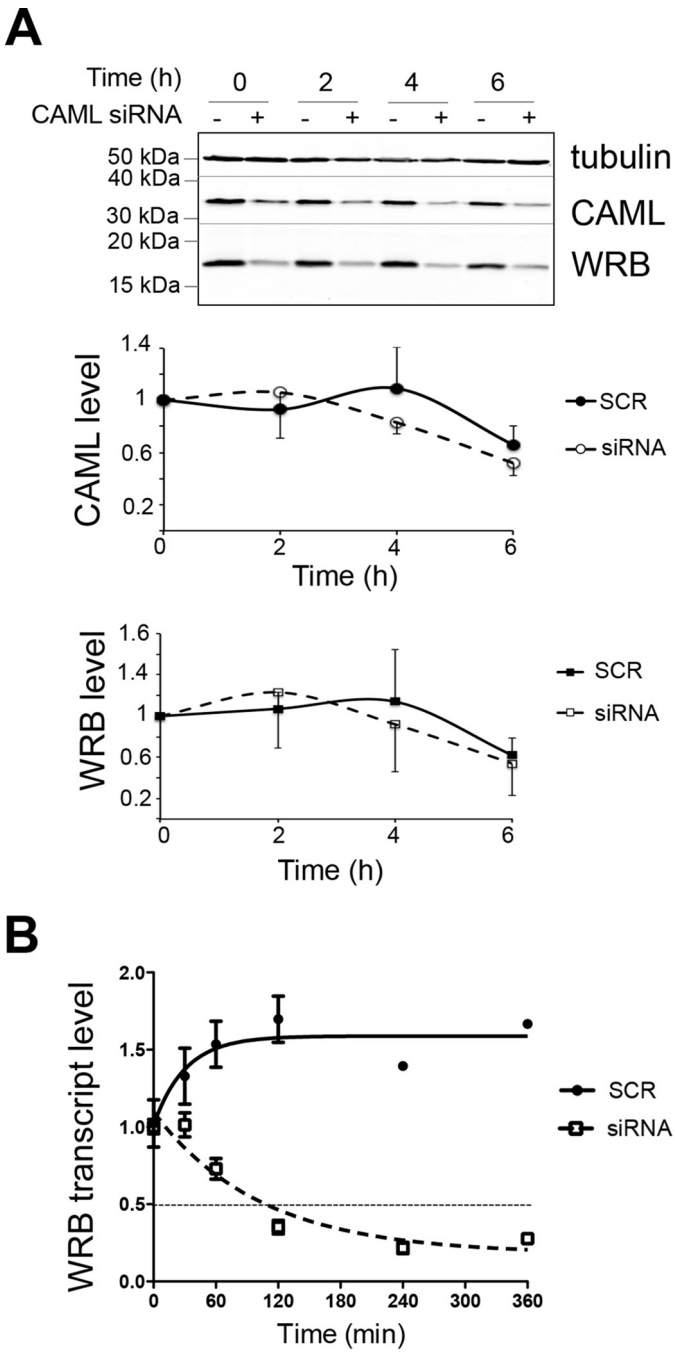

FIGURE 8. **Depletion of CAML destabilizes the WRB transcript but not the encoded protein.** HeLa cells were transfected with CAML silencing (siRNA2) or scrambled (*SCR*) paired oligonucleotides (*A* and *B*). *A*, After 24 h of transfection, cells were incubated with 50 μg/ml CHX for the indicated times and then lysed and analyzed by Western blotting. A representative blot is shown in the *upper panel*. The graphs display mean values ± half range of CAML and WRB band intensities normalized to tubulin and relative to the values at time 0 (n = 2). *B*, after 28 h of transfection, cells were incubated for the indicated times with 60 μM DRB. RNA, extracted from the cell lysates at each time point, was subjected to retrotranscription and qPCR for the WRB transcript. Shown are the averages ± S.D. of two independent experiments, each analyzed in triplicate, normalized to GAPDH levels, and expressed relative to time 0 (= 1).

Previous work has demonstrated that the WRB-CAML complex is sufficient to restore TA protein insertion in Get1/2-deleted yeast cells (22). To investigate whether these proteins alone are able to support TRC40-dependent TA protein insertion, we incorporated the *in vitro* synthesized proteins into

liposomes and found that indeed they generated functional vesicles. The interpretation of our finding is, however, limited by the observation that the amounts of CAML-WRB required to generate functional vesicles were vastly superior to those present in native MRs or in vesicles reconstituted with the eluted fraction. The inefficiency of the *in vitro* synthesized proteins to reconstitute activity could be due to inefficient complex formation; indeed, using anti-CAML antibodies, we were unable to demonstrate co-precipitation of WRB with CAML from the reconstituted PrLs, indicating that most of the incorporated proteins were not associated with each other.[4] Alternatively, we considered the possibility that additional components present in the DBC extract facilitate TA protein insertion. We, therefore, attempted to identify by mass spectrometry such facilitating components among the complex mixture of other microsomal TRC40-interacting proteins. However, this analysis has failed so far to reveal any additional functional component.[4]

In a previous study (23) it was reported that overexpression of either CAML or WRB alone inhibits TA protein insertion, whereas the two subunits overexpressed together are without effect. The inhibitory effect of WRB or CAML was interpreted to be due to competition for TRC40-substrate complexes between the non-functional excess subunits and the functional endogenous receptor. Here, we investigated the effect of altering the CAML-WRB ratio in two different settings. First, in reconstituted PrLs, we were able to systematically alter the amounts of each reconstituted subunit. Second, we used fetal fibroblasts from DS subjects as a possible natural model for CAML-WRB imbalance. Indeed, WRB is encoded in a gene on chromosome 21, and previous studies demonstrated that its transcript is among those that are 1.5-fold up-regulated in DS cells (39, 40); however, WRB protein levels had not been investigated up till now. We found that in primary fibroblasts, WRB protein is up-regulated similarly to its transcript, resulting in a ~1.5-fold increased ratio of WRB to CAML.

In both the PrL and the fibroblast models, alteration of the CAML to WRB ratio did not affect TA protein insertion. Furthermore, when we determined by quantitative Western blotting the absolute amounts of the receptor subunits in microsomes and cells, we found that CAML is present in an ~5-fold molar excess over WRB, suggesting that TA protein insertion does not depend on a strict stoichiometric relationship between the two TRC40 receptor subunits.

The lack of a 1:1 stoichiometry between CAML and WRB raises the problem of the function of the excess CAML. We could not determine whether the excess is associated with WRB in a supercomplex or, rather, exists in a WRB-free pool. Indeed, although our coprecipitation experiments with anti-CAML antibodies demonstrated that WRB is quantitatively associated with CAML, we could not carry out the reverse experiment, because there are currently no available antibodies that immunoprecipitate native WRB. It is possible that some of the many functions linked to CAML, including signal transduction (41, 42), immune cell survival (26), membrane traffic (24, 43), and chromosome segregation (44), are independent from its role in TA protein insertion and could be carried out by a pool of WRB-free CAML. In addition, or alternatively, the excess CAML could increase the efficiency of recruitment of TRC40-TA complexes to the ER membrane, handing them over to the CAML-WRB complex. This hypothesis is supported by our observation that in the reconstituted system, excess CAML stimulated TA protein insertion (Fig. 5). The stimulatory role of excess CAML might recall the one of the low affinity plasma membrane growth factor receptors, which increase the concentration of the ligand in the vicinity of their less abundant, high affinity receptor (45).

It is worth highlighting that the absolute amounts of the two TRC40 receptor subunits determined in our analyses were quite low; in rat liver MRs, we estimated the concentration of WRB to be ~3 pmol/mg of protein, ~1/20,000 of microsomal proteins, and about ½ its estimated concentration in yeast (19). Our estimates for IMR32 and primary human fibroblasts were similar. The low concentration of WRB might seem unexpected given the relatively large number of TA proteins that must be inserted into the ER (6) and considering that WRB's ligand, TRC40, is an abundant protein whose concentration in the rabbit reticulocyte lysate has been estimated at 20–50 nM (8). However, if we consider the situation for the co-translational translocation system, our result with WRB is not that surprising. Indeed, the signal recognition particle receptor is estimated at 16–32 pmol/mg rough microsomal protein (46), 5–10 times more abundant than WRB. Considering that the co-translational system handles, with the exclusion of TA proteins, all polypeptides, membrane and lumenal, destined to the secretory pathway, the concentration of WRB that we found appears entirely consistent with its relatively small workload.

Reciprocal Influence of CAML and WRB on Each Other's Levels—In *Saccharomyces,* Get1 and -2 are expressed in an approximately equimolar ratio, and deletion of one subunit of the complex results in depletion of the other one (19). We investigated whether there is a similar reciprocal influence of the TRC40 receptor subunits and indeed observed that silencing of one subunit caused parallel depletion of the other one. Our initial hypothesis that each subunit is unstable in the absence of the other one was difficult to reconcile with the 5:1 stoichiometry of CAML to WRB. To gain more insight into the phenomenon, we determined the levels of the transcript of each subunit after silencing the other one. Quite remarkably, we found that silencing of each subunit caused a diminution of the levels not only of the targeted mRNA but also of the mRNA for the other subunit. This effect was most marked after CAML silencing; the smaller effect of WRB silencing on CAML transcript levels may be due to the slower time course of the siRNA-mediated knockdown (72 *versus* 48 h for maximal WRB and CAML silencing, respectively).

To investigate whether the reduced mRNA and protein levels driven by silencing of the partner subunit were caused by increased degradation of the transcript and/or the polypeptide product, we analyzed mRNA and protein stability after inhibition of transcription or translation. We carried out this analysis after CAML silencing, because of its pronounced effects on WRB transcript levels. Quite strikingly, we found that WRB protein stability was not affected by CAML depletion, whereas stability of the mRNA was dramatically reduced. Thus, depletion of WRB protein by CAML silencing is an effect secondary

to destabilization of its mRNA and compatible with the imbalance in the stoichiometry of the subunits.

Very recently, a phenomenon similar to the one observed here was reported for the two subunits of a heteromeric K^+ channel expressed in cardiomyocytes, where silencing of one subunit caused a parallel decrease in the transcript for the other one (47). In that study, transcript stability was not investigated, but very interestingly, it was found that the two subunit mRNAs are physically associated and that this association is not dependent on the presence of the nascent-encoded proteins. The authors hypothesized that specific RNA-binding proteins mediate the association of transcripts that code for the subunits of oligomeric complexes, thus facilitating subunit assembly and driving co-regulation of transcript levels.

It is possible that a mechanism similar to the one described for the cardiomyocyte K^+ channel operates also for the CAML and WRB transcripts. As suggested by our reconstitution experiments, the two TRC40 receptor subunits synthesized independently assemble inefficiently *in vitro*; efficient receptor assembly in cells could require the physical proximity of the subunit mRNAs. Whether or not the CAML and WRB transcripts are physically associated, the reciprocal control they exert on each other's intracellular levels represents a novel regulatory mechanism that will undoubtedly be the focus of future investigations.

Author Contributions—S. F. C. conceived the study, carried out or supervised the experiments, and critically revised the manuscript. S. C. carried out the experiments of Fig. 6 and the qPCR analyses of Figs. 7 and 8. A. M. collaborated with S. C. for the qPCR determinations. A. V. carried out the experiment illustrated in Fig. 3. P. S. carried out mass spectrometry analysis. A. C. carried out the experiment illustrated in Fig. 5. R. F. B. provided reagents, discussed the results, and critically revised the manuscript. R. B. designed and supervised the qPCR experiments and contributed under "Discussion." N. B. conceived and coordinated the study and wrote the manuscript. All authors reviewed the results and approved the final version of the manuscript.

Acknowledgments—In addition to the colleagues who provided us with reagents listed under "Experimental Procedures," we are particularly grateful to Fabio Vilardi (University of Goettingen) for his generous contribution of plasmids and antibodies and to Lucio Nitsch (University of Naples Federico II) for providing us with primary cultures of fetal fibroblasts. We thank Bruna Costa for advice on the WRB silencing experiment and Anna Longatti for assistance in the preparation of recombinant protein standards.

References

1. Rapoport, T. A. (2007) Protein translocation across the eukaryotic endoplasmic reticulum and bacterial plasma membranes. *Nature* **450,** 663–669
2. Shao, S., and Hegde, R. S. (2011) Membrane protein insertion at the endoplasmic reticulum. *Annu. Rev. Cell Dev. Biol.* **27,** 25–56
3. Borgese, N., and Fasana, E. (2011) Targeting pathways of C-tail-anchored proteins. *Biochim. Biophys. Acta* **1808,** 937–946
4. Borgese, N. (2015) Membrane Insertion of Tail-anchored Proteins. Wiley Online Library, 10.1002/9780470015902.a0021876.pub2
5. Johnson, N., Powis, K., and High, S. (2013) Post-translational translocation into the endoplasmic reticulum. *Biochim. Biophys. Acta* **1833,** 2403–2409
6. Kalbfleisch, T., Cambon, A., and Wattenberg, B. W. (2007) A bioinformatics approach to identifying tail-anchored proteins in the human genome. *Traffic* **8,** 1687–1694
7. Borgese, N., and Righi, M. (2010) Remote origins of tail-anchored proteins. *Traffic* **11,** 877–885
8. Stefanovic, S., and Hegde, R. S. (2007) Identification of a targeting factor for post-translational membrane protein insertion into the ER. *Cell* **128,** 1147–1159
9. Favaloro, V., Spasic, M., Schwappach, B., and Dobberstein, B. (2008) Distinct targeting pathways for the membrane insertion of tail-anchored (TA) proteins. *J. Cell Sci.* **121,** 1832–1840
10. Schuldiner, M., Metz, J., Schmid, V., Denic, V., Rakwalska, M., Schmitt, H. D., Schwappach, B., and Weissman, J. S. (2008) The GET complex mediates insertion of tail-anchored proteins into the ER membrane. *Cell* **134,** 634–645
11. Hegde, R. S., and Keenan, R. J. (2011) Tail-anchored membrane protein insertion into the endoplasmic reticulum. *Nat. Rev. Mol. Cell Biol.* **12,** 787–798
12. Chartron, J. W., Clemons, W. M., Jr., and Suloway, C. J. (2012) The complex process of GETting tail-anchored membrane proteins to the ER. *Curr. Opin. Struct. Biol.* **22,** 217–224
13. Denic, V., Dötsch, V., and Sinning, I. (2013) Endoplasmic reticulum targeting and insertion of tail-anchored membrane proteins by the GET pathway. *Cold Spring Harb. Perspect. Biol.* **5,** a013334
14. Denic, V. (2012) A portrait of the GET pathway as a surprisingly complicated young man. *Trends Biochem. Sci.* **37,** 411–417
15. Mateja, A., Szlachcic, A., Downing, M. E., Dobosz, M., Mariappan, M., Hegde, R. S., and Keenan, R. J. (2009) The structural basis of tail-anchored membrane protein recognition by Get3. *Nature* **461,** 361–366
16. Bozkurt, G., Stjepanovic, G., Vilardi, F., Amlacher, S., Wild, K., Bange, G., Favaloro, V., Rippe, K., Hurt, E., Dobberstein, B., and Sinning, I. (2009) Structural insights into tail-anchored protein binding and membrane insertion by Get3. *Proc. Natl. Acad. Sci. U.S.A.* **106,** 21131–21136
17. Mateja, A., Paduch, M., Chang, H. Y., Szydlowska, A., Kossiakoff, A. A., Hegde, R. S., and Keenan, R. J. (2015) Protein targeting: structure of the Get3 targeting factor in complex with its membrane protein cargo. *Science* **347,** 1152–1155
18. Jonikas, M. C., Collins, S. R., Denic, V., Oh, E., Quan, E. M., Schmid, V., Weibezahn, J., Schwappach, B., Walter, P., Weissman, J. S., and Schuldiner, M. (2009) Comprehensive characterization of genes required for protein folding in the endoplasmic reticulum. *Science* **323,** 1693–1697
19. Mariappan, M., Mateja, A., Dobosz, M., Bove, E., Hegde, R. S., and Keenan, R. J. (2011) The mechanism of membrane-associated steps in tail-anchored protein insertion. *Nature* **477,** 61–66
20. Stefer, S., Reitz, S., Wang, F., Wild, K., Pang, Y. Y., Schwarz, D., Bomke, J., Hein, C., Löhr, F., Bernhard, F., Denic, V., Dötsch, V., and Sinning, I. (2011) Structural basis for tail-anchored membrane protein biogenesis by the Get3-receptor complex. *Science* **333,** 758–762
21. Wang, F., Whynot, A., Tung, M., and Denic, V. (2011) The mechanism of tail-anchored protein insertion into the ER membrane. *Mol. Cell* **43,** 738–750
22. Vilardi, F., Stephan, M., Clancy, A., Janshoff, A., and Schwappach, B. (2014) WRB and CAML are necessary and sufficient to mediate tail-anchored protein targeting to the ER membrane. *PLoS ONE* **9,** e85033
23. Yamamoto, Y., and Sakisaka, T. (2012) Molecular machinery for insertion of tail-anchored membrane proteins into the endoplasmic reticulum membrane in mammalian cells. *Mol. Cell* **48,** 387–397
24. Tran, D. D., Russell, H. R., Sutor, S. L., van Deursen, J., and Bram, R. J. (2003) CAML is required for efficient EGF receptor recycling. *Dev. Cell* **5,** 245–256
25. Edgar, C. E., Lindquist, L. D., McKean, D. L., Strasser, A., and Bram, R. J. (2010) CAML regulates Bim-dependent thymocyte death. *Cell Death Differ.* **17,** 1566–1576
26. Chan, S. L., Lindquist, L. D., Hansen, M. J., Girtman, M. A., Pease, L. R., and Bram, R. J. (2015) Calcium-modulating cyclophilin ligand is essential for the survival of activated T cells and for adaptive immunity. *J. Immunol.* **195,** 5648–5656
27. Brambillasca, S., Yabal, M., Makarow, M., and Borgese, N. (2006) Unas-

sisted translocation of large polypeptide domains across phospholipid bilayers. *J. Cell Biol.* **175,** 767–777
28. Colombo, S. F., Longhi, R., and Borgese, N. (2009) The role of cytosolic proteins in the insertion of tail-anchored proteins into phospholipid bilayers. *J. Cell Sci.* **122,** 2383–2392
29. Vilardi, F., Lorenz, H., and Dobberstein, B. (2011) WRB is the receptor for TRC40/Asna1-mediated insertion of tail-anchored proteins into the ER membrane. *J. Cell Sci.* **124,** 1301–1307
30. Holloway, M. P., and Bram, R. J. (1998) Co-localization of calcium-modulating cyclophilin ligand with intracellular calcium pools. *J. Biol. Chem.* **273,** 16346–16350
31. Adamus, G., Arendt, A., and Hargrave, P. A. (1991) Genetic control of antibody response to bovin rhodopsin in mice: epitope mapping of rhodopsin structure. *J. Neuroimmunol.* **34,** 89–97
32. Yu, Y. H., Sabatini, D. D., and Kreibich, G. (1990) Antiribophorin antibodies inhibit the targeting to the ER membrane of ribosomes containing nascent secretory polypeptides. *J. Cell Biol.* **111,** 1335–1342
33. Harlow, E., and Lane, D. (1988) *Antibodies: A Laboratory Manual*, pp. 522–523, Cold Spring Harbor Laboratory Press, Cold Spring Harbor, NY
34. Brambillasca, S., Yabal, M., Soffientini, P., Stefanovic, S., Makarow, M., Hegde, R. S., and Borgese, N. (2005) Transmembrane topogenesis of a tail-anchored protein is modulated by membrane lipid composition. *EMBO J.* **24,** 2533–2542
35. Nicchitta, C. V., Migliaccio, G., and Blobel, G. (1991) Biochemical fractionation and assembly of the membrane components that mediate nascent chain targeting and translocation. *Cell* **65,** 587–598
36. Görlich, D., and Rapoport, T. A. (1993) Protein translocation into proteoliposomes reconstituted from purified components of the endoplasmic reticulum membrane. *Cell* **75,** 615–630
37. Brambillasca, S., Altkrueger, A., Colombo, S. F., Friederich, A., Eickelmann, P., Mark, M., Borgese, N., and Solimena, M. (2012) CDK5 regulatory subunit-associated protein 1-Like 1 (CDKAL1) is a tail-anchored protein in the endoplasmic reticulum (ER) of insulinoma cells. *J. Biol. Chem.* **287,** 41808–41819
38. Korenberg, J. R., Chen, X. N., Schipper, R., Sun, Z., Gonsky, R., Gerwehr, S., Carpenter, N., Daumer, C., Dignan, P., and Disteche, C. (1994) Down syndrome phenotypes: the consequences of chromosomal imbalance. *Proc. Natl. Acad. Sci. U.S.A.* **91,** 4997–5001
39. Prandini, P., Deutsch, S., Lyle, R., Gagnebin, M., Delucinge Vivier, C., Delorenzi, M., Gehrig, C., Descombes, P., Sherman, S., Dagna Bricarelli, F., Baldo, C., Novelli, A., Dallapiccola, B., and Antonarakis, S. E. (2007) Natural gene-expression variation in Down syndrome modulates the outcome of gene-dosage imbalance. *Am. J. Hum. Genet.* **81,** 252–263
40. Conti, A., Fabbrini, F., D'Agostino, P., Negri, R., Greco, D., Genesio, R., D'Armiento, M., Olla, C., Paladini, D., Zannini, M., and Nitsch, L. (2007) Altered expression of mitochondrial and extracellular matrix genes in the heart of human fetuses with chromosome 21 trisomy. *BMC Genomics* **8,** 268
41. Bram, R. J., and Crabtree, G. R. (1994) Calcium signalling in T cells stimulated by a cyclophilin B-binding protein. *Nature* **371,** 355–358
42. Guo, S., Lopez-Ilasaca, M., and Dzau, V. J. (2005) Identification of calcium-modulating cyclophilin ligand (CAML) as transducer of angiotensin II-mediated nuclear factor of activated T cells (NFAT) activation. *J. Biol. Chem.* **280,** 12536–12541
43. Yuan, X., Yao, J., Norris, D., Tran, D. D., Bram, R. J., Chen, G., and Luscher, B. (2008) Calcium-modulating cyclophilin ligand regulates membrane trafficking of postsynaptic $GABA_A$ receptors. *Mol. Cell. Neurosci.* **38,** 277–289
44. Liu, Y., Malureanu, L., Jeganathan, K. B., Tran, D. D., Lindquist, L. D., van Deursen, J. M., and Bram, R. J. (2009) CAML loss causes anaphase failure and chromosome missegregation. *Cell Cycle* **8,** 940–949
45. Couchman, J. R. (2003) Syndecans: proteoglycan regulators of cell-surface microdomains? *Nat. Rev. Mol. Cell Biol.* **4,** 926–937
46. Guth, S., Völzing, C., Müller, A., Jung, M., and Zimmermann, R. (2004) Protein transport into canine pancreatic microsomes: a quantitative approach. *Eur. J. Biochem.* **271,** 3200–3207
47. Liu, F., Jones, D. K., de Lange, W. J., and Robertson, G. A. (2016) Cotranslational association of mRNA encoding subunits of heteromeric ion channels. *Proc. Natl. Acad. Sci. U.S.A.* **113,** 4859–4864